Journal of the Serbian Chemical Society
JSCS-info@shd.org.rs • www.shd.org.rs/JSCS

J. Serb. Chem. Soc. 85 (8) 1021–1032 (2020)
JSCS–5356

UDC 547.857.7:532.14+546.311+
544.354–128.4:533.912
Original scientific paper

Properties of the excited electronic states of guanine quartet complexes with alkali metal cations

BRANISLAV Ž. MILOVANOVIĆ#, MILENA M. PETKOVIĆ#
and MIHAJLO R. ETINSKI*#

University of Belgrade, Faculty of Physical Chemistry, Studentski trg 12–16, 11158 Belgrade, Serbia

(Received 25 October, revised 2 December, accepted 24 December 2019)

Abstract: G-quartets are supra-molecular structures that consist of four guanine molecules connected by eight hydrogen bonds. They are additionally stabilized by metal cations. In this contribution, the excited states of G-quartet and its complexes with lithium, sodium and potassium were studied by employing time-dependent density functional theory. The findings indicate that vertical excitations from the optimized ground state involve transitions from several bases, whereas excitations from the optimized lowest excited state include transitions from one base. The charge-transfer character of these states was analyzed. It was shown that the cations are able to modify positions of the maxima of the fluorescence spectra of the complexes.

Keywords: density functional theory; G-quadruplex; fluorescence.

INTRODUCTION

Self-assembly of guanines leads to formation of square planar G-quartets (G_4) which might further stack into G-quadruplexes. These supramolecular structures allow binding of metal cations into the central cavity that results in more stable cation-templated structures. The molecular structure of a G-quartet/metal cation complex is displayed in Fig. 1. The stability of the complex is largely determined by cation–guanine interaction and Hoogsteen and/or bifurcated hydrogen bonding between hydrogen bond donating and accepting groups. It is believed that hydrogen bonding accounts for 50 % of the energy responsible for internal stability of these structures.[1]

G-quartets are highly selective towards metal cations. In an aqueous solution, alkali metal stabilization is in the order: $Cs^+ > Rb^+ > K^+ > Na^+ > Li^+$, while in the gas phase, the affinities are in the reversed order.[2] This is a con-

* Corresponding author. Email: etinski@ffh.bg.ac.rs
# Serbian Chemical Society member.
https://doi.org/10.2298/JSC191025140M

sequence of the increasing alkali metal dehydration as going from Li^+ to Cs^+.[2,3] It is additionally due to the fact that smaller cations have stronger electrostatic interactions and thus they reduce the repulsion between oxygen atoms of the guanines.[4] Zaccaria and Fonseca Guerra argued that this mutual repulsion of the oxygens appears to be a secondary effect and thus the cation is primarily required for the enthalpic stabilization of these complexes.[5] Some authors[6,7] considered cation–oxygen interaction to be mostly electrostatic in nature whereas others[1,8] considered it to be covalent.

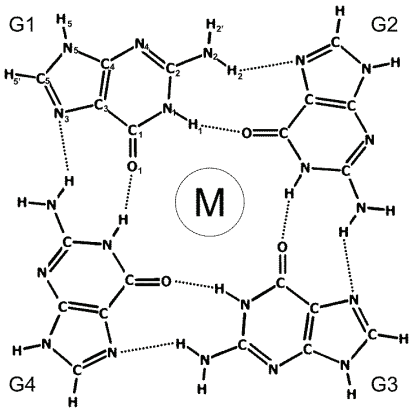

Fig. 1. Atomic and fragment numbering of the G_4–M complex.

Although excited states of G-quadruplexes were investigated both experimentally[9–13] and theoretically,[14,15] not much is known about how cations tune their properties. Hua and co-workers showed that alkali metal cations (Na^+ and K^+) play an important role in modulating decay pathways of G-quadruplexes.[12] In the presence of a potassium cation, G-quadruplex emission stems from excitonic $\pi\pi^*$ states, whereas in the presence of a sodium cation, the emission originates from charge-transfer (CT) states. Hua and coworkers argued that such difference is not due to the original excited electronic states but is a consequence of different mobility of potassium and sodium cations during electronic relation. Improta studied the excited states of the G-quartet with two potassium cations at the M05-2X/6-31G(d) level of theory.[14] He found that the lowest absorption peak of hydrated guanosine monophosphate at approximately 4.90 eV originates from two $\pi\pi^*$ states. The lowest energy transition assigned to the L_a state originates from HOMO to LUMO transition, whereas the higher energy state is the L_b state, which stems from HOMO to LUMO+1 excitation. Although the energy difference and relative intensities of these two states were correctly reproduced with the M05-2X functional, there was a blue-shift of 0.86 eV with respect to the experimental energies. This energy difference was attributed to the employed basis set and the lack of solvent–solute interaction as well as vibronic effects in the employed computational model.

In this contribution, the extent to which alkali metal cations modulate low--lying excited singlet electronic states and their charge-transfer character in G-quartet complexes with metal cations were systematically examined. The goal was to determine whether various monovalent metal cations might change the charge-transfer content of the lowest excited singlet state in its minimum. To this end, the ground and lowest excited singlet electronic states of G-quartet complexes with lithium, sodium and potassium cations were optimized and a detailed analysis of their charge-transfer character performed.

COMPUTATIONAL DETAILS

The ground state geometries of the G_4–M complexes were optimized with the M06-2X functional,[16] which correctly describes the dispersion interactions important for hydrogen bond description. The excited states were computed using the time-dependent density functional theory with a long-range corrected CAM-B3LYP functional.[17,18] This functional provides a balance description of local and charge-transfer states. It also outperforms the M06-2X functional in the energy values of the excited state.[19] Split valence 6-31+G(d,p) and 6-31G basis sets[20–24] were employed for the ground and excited state optimizations, respectively. Vertical excitation spectra were calculated with cc-pVDZ correlation consistent basis set[25] for guanines and TZVP basis set[26] for the metal cations. Geometry optimizations were performed without symmetry restrictions. All electronic structure calculations were realized using the Gaussian 16 program package.[27]

Characterization of excited state properties was performed by employing the Multiwfn program.[28,29] The interfragment charge transfer (IFCT) methodology was applied and the natural transition orbitals (NTOs) computed. The IFCT method is based on the analysis of the transition density matrix. This matrix is used to obtain the interfragment charge transfer matrix *M*, the diagonal elements of which represent the magnitude of electron redistribution on a particular atom in the corresponding excited state upon excitation from the ground state. The off-diagonal elements represent the magnitude of the electron redistribution between different atoms (*i.e.*, fragments if block matrices are considered). By summing up certain values of these matrix elements, the local excitation and charge-transfer content (in fractions) for predefined fragments in the system could be estimated for each excited state. Thus, the following descriptor was defined:

$$X = \frac{\sum_{i,j\in(G_k,M\rightarrow G_l,M)} M_{ij}}{\sum_{i,j} M_{ij}} \quad (1)$$

The sum in the denominator in Eq. (1) runs over all matrix elements while the sum in the numerator defines the quantity *X* as follows: *X* represents local excitation (LE) content if *i* and *j* run over block diagonal matrices that represent only the contribution of excitations within each fragment (single guanine unit, G_l, G_k = 1, 2, 3, 4; see Fig 1.) and metal ion (M), *i.e.*, G1→G1, G2→G2, G3→G3, G4→G4 and M→M; X represents the charge-transfer content if summing all block non-diagonal elements, for example, contribution from G1→M or G4→G3. The charge-transfer content can be divided into three parts: $CT_{neighbor}$, if only charge-transfer excitation contributions between the neighboring fragments are considered, *i.e.*, G1→G2, G1→G4; $CT_{diagonal}$ if contributions are only between diagonal guanine frag-

ments G1, G3 and G2, G4; CT_{metal} depicting the charge transfer between guanines and metal ion. The descriptors satisfy the following equation:

$$LE + CT = LE + CT_{neighbour} + CT_{diagonal} + CT_{metal} = 1 \quad (2)$$

RESULTS AND DISCUSSION

The ground state geometry

The optimized structures of G_4, G_4–Li^+, G_4–Na^+, G_4–K^+ are presented in Fig. 2 (additional data are given as Supplementary material to this paper). Their most important geometrical parameters are collected in Table I. The G_4 structure is almost planar and it has the C_{4h} symmetry group. The average distance between oxygen atoms and their geometrical center is 2.95 Å. The N_1–$H_1\cdots O_1$ and N_2–$H_2\cdots N_3$ hydrogen bond lengths amount to 1.91 and 2.46 Å, respectively. Alkali metal cations have a significant impact on the structure of the complexes. The presence of the cations decreases the repulsion between the oxygen atoms and thus decreases the lengths of the hydrogen bond. The later effect results in stronger hydrogen bonds. In addition, different cationic radii are responsible for different geometrical parameters of the complexes. The G_4–Li^+ geometry is close to the S_4 symmetry group. The average distance between the oxygen atom and lithium cation is 1.99 Å. The N_1–$H_1\cdots O_1$ and N_2–$H_2\cdots N_3$ hydrogen bond lengths are equal to 1.99 and 1.83 Å, respectively.

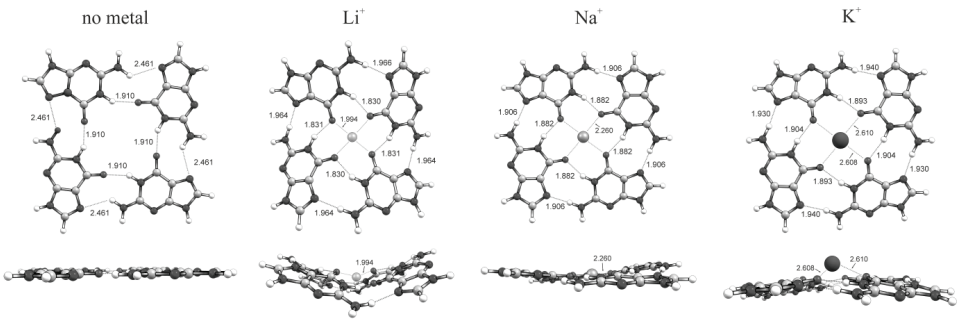

Fig. 2. The G_4 and G_4–M (M = Li^+, Na^+, K^+) structures with top and side view. The indicated hydrogen bond lengths and O_1–M distances are given in Å.

The dihedral angle between the oxygen atoms has a value of 35.2°, indicating a highly twisted structure. The G_4–Na^+ structure is much less distorted compared to the G_4–Li^+ one and it has approximately S_4 group symmetry. Dihedral angle between the oxygen atoms is equal to 0.4°. The N_1–$H_1\cdots O_1$ and N_2–$H_2\cdots N_3$ bond lengths increase and decrease relative to those of the complex with lithium cation, respectively. The structure with potassium cation has similar properties to those of the complex with sodium cation. The symmetry of the G_4-K^+ geometry is close to that of the C_4 group. Smaller ionic radius of Li^+ and

Na^+ allow these ions to be positioned in or near the center of the G_4 structure, whereas K^+ is located out of the plane defined by the G_4 structure (see Fig. 2).

TABLE I. Geometrical parameters for G_4 and G_4–M (M=Li^+, Na^+, K^+) structures

Structure	Bond distance, Å			Bond angle, °		
	d[O_1–M][a]	N_1–H_1···O_1[b]	N_2–H_2···N_3[c]	∠$N_1H_1O_1$[d]	∠$N_2H_2N_3$[e]	dih_{OOOO}[f]
G_4	2.95	1.91	2.46	151.7	131.8	0.4
G_4–Li^+	1.99	1.83	1.96	152.6	167.7	35.2
G_4–Na^+	2.26	1.88	1.91	161.8	176.2	0.4
G_4–K^+	2.61	1.90	1.93	168.1	170.4	1.1

[a]Average distance between four oxygen atoms and alkali metal ion. For an empty G_4 scaffold, the average distance of the O_1-geometrical center is taken; [b]average inner hydrogen bond distance; [c]average outer hydrogen bond distance; [d]average inner hydrogen bond angle; [e]average outer hydrogen bond angle; [f]dihedral angle defined by the four O_1 oxygen atoms

Vertical excitation spectrum

Vertical excitation energies, oscillatory strengths, excited state descriptors and fragment contributions to excitations of the first eight states of G_4 and G_4–M complexes are collected in Table II. Electronic coupling and degeneracy of the excited states of the multiple guanine bases in the examined systems is responsible for presence of the delocalized states in these supramolecular structures. Many different canonical orbitals contribute to electronic transitions and thus it is difficult to understand how the electron density is modified upon excitations. On the other hand, natural transition orbitals provide a compact description of the electronic excitations and a small number of orbitals are needed to describe the transitions. The lowest four states are the combination of different monomer-like L_a transitions, whereas the next four states belong to monomer-like L_b transitions. Although the transitions include charge-transfer, there is no net charge separation.

The G_4 absorption spectrum has two distinct maxima located at 5.22 and 5.65 eV. The exciton coupling is found to be less than 0.01 eV. Only the first state of the L_a transition is stabilized by 0.04 eV with respect to the other three states. The lowest absorption band originates from transitions to the bright S_2 and S_3 states, which are delocalized over the diagonal guanine monomers G1, G3 and G2, G4, respectively. Local excitations contribute to half of all the transitions. The dominant CT contributions are diagonal, whereas the excitations between neighboring guanine monomers account for only 7 %. The S_1 and S_4 states are dark states and thus do not contribute to this absorption band. These two states stem from the orbitals that are delocalized over all the guanine monomers. Their excitations have mostly neighboring CT character. The four L_b states have similar properties to those of the L_a states but in this case, the dark states are the third and four states in the L_b group.

TABLE II. Vertical excitation energies, oscillator strengths, excited state descriptors and fragment contributions to excitations of G_4 and G_4–M (M = Li^+, Na^+, K^+) complexes

Complex	State	E / eV	f	LE	CT	$CT_{neighbour}$	$CT_{diagonal}$	CT_{metal}	Fragment contributions
G_4	S_1	5.19	0.00	0.250	0.750	0.500	0.250	–	20% G1234 →G1234 + 24% G13→G13 + 24% G24→G24 + 27% G1234→G1234
	S_2	5.23	0.36	0.465	0.535	0.070	0.465	–	46% G1→G1 + 46% G3→G3
	S_3	5.23	0.36	0.465	0.535	0.070	0.465	–	46% G2→G2 + 46% G4→G4
	S_4	5.23	0.00	0.250	0.750	0.500	0.250	–	22% G1234 →G1234 + 24% G24→G24 + 24% G13→G13 + 26% G1234→G1234
	S_5	5.65	0.80	0.370	0.630	0.261	0.370	–	41% G4→G4 + 42% G2→G2
	S_6	5.65	0.80	0.370	0.630	0.260	0.370	–	41% G1→G1 + 42% G3→G3
	S_7	5.65	0.00	0.250	0.750	0.500	0.250	–	22% G1234→G1234 + 24% G13→G13 + 24% G24→G24 + 26% G1234→G1234
	S_8	5.66	0.00	0.250	0.750	0.500	0.250	–	22% G1234→G1234 + 24% G13→G13 + 24% G24→G24 + 26% G1234→G1234
G_4–Li^+	S_1	5.03	0.02	0.248	0.752	0.495	0.247	0.010	21% G1234→G1234 + 23% G24→G24 + 23% G13→G13 + 28% G1234→G1234
	S_2	5.06	0.29	0.466	0.534	0.058	0.466	0.010	45% G13→G13 + 49% G13→G13
	S_3	5.06	0.29	0.466	0.534	0.058	0.466	0.010	45% G24→G24 + 49% G24→G24
	S_4	5.14	0.00	0.248	0.752	0.495	0.248	0.009	21% G1234→G1234 + 23% G13→G13 + 23% G24→G24 + 28% G1234→G1234
	S_5	5.64	0.00	0.249	0.751	0.498	0.249	0.003	24% G1234→G1234 + 24% G13→G13 + 24% G24→G24 + 25% G1234→G1234
	S_6	5.69	0.66	0.472	0.528	0.052	0.472	0.003	47% G24→G24 + 47% G24→G24
	S_7	5.69	0.66	0.472	0.528	0.052	0.472	0.003	45% G13→G13 + 49% G13→G13
	S_8	5.73	0.13	0.249	0.751	0.498	0.249	0.003	21% G1234→G1234 + 24% G24→G24 + 24% G13→G13 + 26% G1234→G1234

TABLE II. Continued

Complex	State	E / eV	f	LE	CT	$CT_{neighbour}$	$CT_{diagonal}$	CT_{metal}	Fragment contributions
G_4–Na^+	S_1	5.00	0.01	0.244	0.756	0.488	0.244	0.022	20% G1234→G1234 + 22% G13→G13 + 22% G24→G24 + 32% G1234→G1234
	S_2	5.03	0.30	0.474	0.526	0.029	0.473	0.023	44% G13→G13 + 52% G13→G13
	S_3	5.03	0.30	0.474	0.526	0.029	0.473	0.023	44% G24→G24 + 52% G24→G24
	S_4	5.10	0.00	0.245	0.755	0.489	0.245	0.020	19% G1234→G1234 + 22% G13→G13 + 22% G24→G24 + 32% G1234→G1234
	S_5	5.64	0.00	0.249	0.751	0.497	0.249	0.005	23% G1234→G1234 + 24% G13→G13 + 24% G24→G24 + 25% G1234→G1234
	S_6	5.69	0.76	0.272	0.728	0.450	0.272	0.005	16% G13→G13 + 22% G13→G13 + 31% G24→G24 + 32% G24→G24
	S_7	5.69	0.76	0.272	0.728	0.450	0.272	0.005	16% G24→G24 + 22% G24→G24 + 31% G13→G13 + 32% G13→G13
	S_8	5.73	0.00	0.249	0.751	0.497	0.249	0.005	19% G1234→ G1234 + 22% G13→G13 + 22% G24→G24 + 32% G1234→G1234
G_4–K^+	S_1	5.02	0.01	0.241	0.759	0.480	0.240	0.035	20% G1234→G1234 + 23% G24→G24 + 23% G13→G13 + 30% G1234→G1234
	S_2	5.04	0.28	0.466	0.534	0.032	0.463	0.036	45% G13→G13 + 50% G13→G13
	S_3	5.04	0.30	0.466	0.534	0.030	0.464	0.038	45% G24→G24 + 50% G24→G24
	S_4	5.09	0.01	0.241	0.759	0.478	0.239	0.038	18% G1234→G1234 + 22% G13→G13 + 22% G24→G24 + 32% G1234→G1234
	S_5	5.63	0.01	0.246	0.754	0.489	0.245	0.018	23% G13→G13 + 24% G24→G24 + 24% G1234→G1234 + 25% G1234→G1234
	S_6	5.68	0.77	0.474	0.526	0.046	0.474	0.006	47% G24→G24 + 48% G24→G24
	S_7	5.68	0.75	0.474	0.526	0.043	0.473	0.008	47% G13→G13 + 47% G13→G13
	S_8	5.71	0.00	0.245	0.755	0.486	0.244	0.020	20% G1234→G1234 + 22% G13→G13 + 24% G24→G24 + 29% G1234→G1234

The presence of alkali metal cations in G-quartet results in a red-shift of the lower energy absorption band. This spectral displacement amounts to 0.17, 0.20 and 0.18 eV for the G4–Li^+, G4–Na^+ and G4–K^+ complexes, respectively. Thus, the cation radiuses are not correlated with the band shift of the L_a state. On the other hand, the cation radiuses correlate with the contribution of the guanine to metal excitations. These contributions are approximately 1, 2 and 3.5 % for the G_4–Li^+, G_4–Na^+ and G_4–K^+ complexes, respectively.

The CT_{metal} contributions mostly arise at the expense of $CT_{neighbour}$ content making the *LE* and $CT_{diagonal}$ components almost unchanged. The L_b states undergo a blue-shift which amounts to less than 0.05 eV in all three cases. Similarly to the L_a states, these shifts are not correlated with the cation radii. The CT_{metal} contribution to L_b states accounts by less than 0.5 % in the G_4–Li^+ and G_4–Na^+ systems and by less than 2.0 % in the G_4–K^+. Metal ions change the ordering of the bright and dark L_b states compared to the empty quartet scaffold. The S_6 and S_7 states become bright states responsible for the high-energy absorption band. The *LE* content is comparable to the one of the L_a states except for the G_4–Na^+ system that has a different character of the S_6 and S_7. The S_6 and S_7 bright L_b states of the G_4–Na^+ system exhibit a high *CT* content that amounts to 72.8 %. The characters of the S_5 and S_8 states are not significantly influenced by the alkali metal ions in the G_4–M complexes and they remain dark with a CT content of 75 %.

The first excited state

The properties of the first excited singlet state are not only important due to their relation with fluorescence but they might also provide insight into the electronic relaxation of the molecule. Hua and co-workers argued that the fluorescence of G-quadruplexes in the presence of sodium and potassium cations originates from states with different charge-transfer properties.[12] It is questionable whether these properties remain for isolated G-quartets, or are a consequence of G-quartet stacking. Adiabatic and vertical excitation energies, oscillator strengths, excited state descriptors and fragment contributions to the S_1 state of G_4 and G_4–M complexes are presented in Table III. The vertical excitation energies correspond to the energy differences between the S_1 and ground state at the optimized geometry of the S_1 state. The optimized geometries of the S_1 states of G_4 and G_4–M complexes are given in Fig. 3, whereas the most important geometric parameters are collected in Table IV. Natural transition orbitals reveal that the electronic excitation is localized on a single guanine fragment so that the transition mostly involves a local excitation. The charge transfer character is very small and it does not change upon cation substitution. Thus, it was concluded that the properties of the S_1 states of G-quartet and G-quadruplex are different. It is proposed that the relaxation of the excited state of G-quartets proceeds *via* guan-

ine monomers and does not include all bases. It is likely that the lifetime of the excited state of the G-quartet is similar to that of an isolated guanine.

TABLE III. Adiabatic and vertical excitation energies, oscillator strengths, excited state descriptors and fragment contributions to the S_1 state of G_4 and G_4–M (M = Li^+, Na^+, K^+) complexes

Structure	E_A eV	E_V eV	f	LE	CT	$CT_{neighbour}$	$CT_{diagonal}$	CT_{metal}	Fragment contributions
G_4	4.97	3.47	0.11	0.979	0.021	0.018	0.003	–	98% G3→G3
G_4–Li^+	4.97	4.43	0.17	0.939	0.061	0.042	0.008	0.010	96% G4→G4
G_4–Na^+	4.96	4.35	0.17	0.938	0.062	0.034	0.007	0.021	97% G2→G2
G_4–K^+	4.89	3.25	0.10	0.944	0.056	0.023	0.005	0.028	99% G2→G2

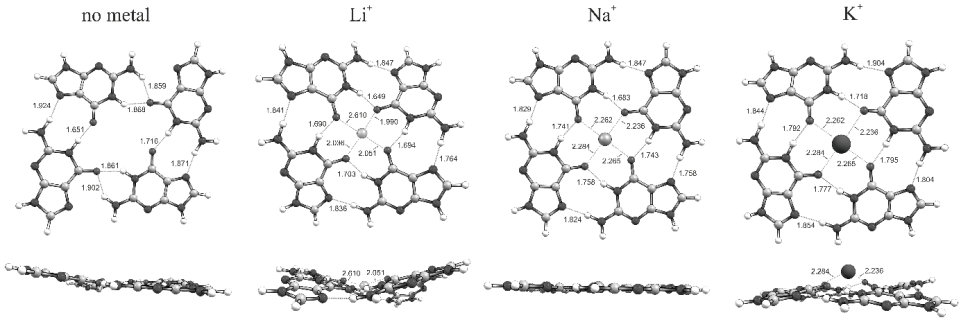

Fig. 3. The structures of G_4 and G_4–M (M = Li^+, Na^+, K^+) of the optimized state of S_1 with top and side view. The indicated hydrogen bond lengths and O1–M distances are given in Å.

The adiabatic energies of G_4, and the G_4–Li^+ and G_4–Na^+ complexes amount to approximately 5 eV. The complex with potassium cation has 0.07–0.08 eV lower adiabatic energy than the other three systems. On the other hand, the vertical excitation energies drastically vary with the cation species. The lowest value (3.25 eV) is found in the complex with potassium cation. The vertical excitation energy of the G_4 complex is 0.22 eV higher. The complexes with lithium and sodium cations have vertical energies that are approximately equal to 4.4 eV.

Therefore, there is a large difference in the maxima of the fluorescence spectra between the examined complexes. These discrepancies are correlated with the differences between optimized geometries of the ground and the first excited states. In addition to Hoogsteen hydrogen bonds, the G_4 structure also exhibits bifurcated hydrogen bonds in the S_1 state, *i.e.*, the O_1 atom is the hydrogen bond acceptor for two bonds. The G_4 geometry loses its planarity in the excited state. The average distance between oxygen atoms and their geometric centers decreases in the excited state by 0.25 Å. Thus, the ground state energy of the G_4 structure is strongly destabilized at the S_1 state optimized geometry. The

complexes with the cations exhibit smaller geometrical changes in the optimized S_1 state than the G_4 structure. Yet, the largest distortions between these complexes are found for the structure with potassium cation – its dihedral angle between the oxygen atoms changes by 5.8 degrees.

TABLE IV. Geometrical parameters for G_4 and G_4–M (M = Li^+, Na^+, K^+) structures in the S_1 optimized state

Structure	Bond distance, Å			Bond angle, °		
	d[O1–M][a]	N1–H1···O1[b]	N2–H2···N3[c]	∠N1H1O1[d]	∠N2H2N3[e]	dih_{OOOO}[f]
G_4	2.70	1.77	2.21	160.6	148.5	–1.6
G_4–Li^+	2.04	1.69	1.82	158.4	170.5	31.5
G_4–Na^+	2.26	1.74	1.81	165.4	174.6	–1.2
G_4–K^+	2.61	1.77	1.85	168.8	170.8	–4.7

[a]Average distance between four oxygen atoms and alkali metal ion. For empty G_4 scaffold average distance of O_1-geometrical center is taken; [b]average inner hydrogen bond distance; [c]average outer hydrogen bond distance; [d]average inner hydrogen bond angle; [e]average outer hydrogen bond angle; [f]dihedral angle defined by the four O_1 oxygen atoms

CONCLUSIONS

G-quartet complexes with alkali metal cations are supramolecular structures stabilized by cation–guanine interaction and hydrogen bonding. Smaller cations are positioned in or close to the plane defined by G-quartet, whereas larger cations are located out of the plane. Due to the degeneracy caused by multiple guanines, the vertical excitations of G-quartet complexes are not localized on one but involve several guanines. It was found that electronic transitions have local excitation and charge-transfer character that includes neighbor and diagonal contributions. Although the transitions include charge-transfer, there is no net charge separation. The lowest four states are found to be the combination of monomer-like L_a excitations, whereas the next four states have monomer-like L_b excitations. In the presence of the alkali cations, the L_a and L_b transitions exhibit red- and blue-shifts, respectively. The shifts are not sensitive to the nature of the cation. The lowest excited singlet state at its minimum is localized on one guanine monomer and its charge-transfer character is approximately equal for all complexes with the cations. The existence of localized excitation implies that the excited state lifetime of the G-quartet is similar to that of an isolated guanine monomer. Although all examined complexes have very similar adiabatic energies, their vertical excitation energies at the S_1 minimum differ considerably. These differences are attributed to distortions of the complex geometries at the S_1 minimum. Consequently, alkali metal cations tune the fluorescence spectra maxima of the G-quartet complexes.

SUPPLEMENTARY MATERIAL

Additional data are available electronically at the pages of journal website: https://www.shd-pub.org.rs/index.php/JSCS/index, or from the corresponding author on request.

Acknowledgements. The research leading to these results was co-funded by the European Commission under the H2020 Research Infrastructures contract No. 675121 (project VI-SEEM). The authors acknowledge the Ministry of Education, Science, and Technological Development of the Republic of Serbia (Contract No. 451-03-68/2020-14/200146) for financial support. We thank Dr. Nađa Došlić for providing a part of computational time. B. Ž. M. acknowledges the Municipality of Arandjelovac (Youth Office) for the financial support.

ИЗВОД

СВОЈСТВА ПОБУЂЕНИХ ЕЛЕКТРОНСКИХ СТАЊА КОМПЛЕКСА КВАРТЕТА ГУАНИНА СА КАТЈОНИМА АЛКАЛНИХ МЕТАЛА

БРАНИСЛАВ Ж. МИЛОВАНОВИЋ, МИЛЕНА. М. ПЕТКОВИЋ и МИХАЈЛО Р. ЕТИНСКИ

Универзитет у Београду – Факултет за физичку хемију, Студентски трг 12–16, 11158 Београд

G-квартети су супра-молекулске структуре које се састоје од четири гунанина повезана помоћу осам водоничних веза. Оне су додатно стабилизоване металним катјонима. У овом раду проучавамо побуђена стања G-квартета и њихових комплекса са литијумом, натријумом и калијумом користећи временски зависну теорију функционала електронске густине. Наши резултати указују да вертикална побуђивања из оптимизованог основног стања укључују прелазе између неколико база, док побуђивања из оптимизованог најниже побуђеног стања укључују прелазе са једне базе. Анализиран је удео преноса наелектрисања у тим стањима. Показали смо да катјони могу да модификују положаје максимума флуоросцентних спектара комплекса.

(Примљено 25. октобра, ревидирано 2. децембра, прихваћено 24. децембра 2019)

REFERENCES

1. Y. P. Yurenko, J. Novotny, V. Sklenávr, R. Marek, *Phys. Chem. Chem. Phys.* **16** (2014) 2072 (https://dx.doi.org/10.1039/C3CP53875C)
2. J. Gu, J. Leszczynski, *J. Phys. Chem., A* **106** (2002) 529 (https://dx.doi.org/10.1021/jp012739g)
3. F. Zaccaria, G. Paragi, C. Fonseca Guerra, *Phys. Chem. Chem. Phys.* **18** (2016) 20895 (https://dx.doi.org/10.1039/C6CP01030J)
4. M. T. Rodgers, P. B. Armentrout, *J. Am. Chem. Soc.* **122** (2000) 8548–8558 (https://dx.doi.org/10.1021/ja001638d)
5. F. Zaccaria, C. Fonseca Guerra, *Chem. - A Eur. J.* **24** (2018) 16315 (https://dx.doi.org/10.1002/chem.201803530)
6. G. Louit, A. Hocquet, M. Ghomi, M. Meyer, J. Sühnel, *PhysChemComm* **6** (2003) 1 (https://dx.doi.org/10.1039/B210911E)
7. J. Gu, J. Leszczynski, M. Bansal, *Chem. Phys. Lett.* **311** (1999) 209 (https://dx.doi.org/10.1016/S0009-2614(99)00821-0)
8. W. S. Ross, C. C. Hardin, *J. Am. Chem. Soc.* **116** (1994) 6070 (https://dx.doi.org/10.1021/ja00093a003)
9. F. Rosu, V. Gabelica, E. De Pauw, R. Antoine, M. Broyer, P. Dugourd, *J. Phys. Chem., A* **116** (2012) 5383 (https://dx.doi.org/10.1021/jp302468x)

10. L. Martinez-Fernández, A. Banyasz, D. Markovitsi, R. Improta, *Chem. - A Eur. J.* **24** (2018) 15185 (https://dx.doi.org/10.1002/chem.201803222)
11. M. E. Sherlock, C. A. Rumble, C. K. Kwok, J. Breffke, M. Maroncelli, P. C. Bevilacqua, *J. Phys. Chem., B* **120** (2016) 5146 (https://dx.doi.org/10.1021/acs.jpcb.6b03790)
12. Y. Hua, P. Changenet-Barret, R. Improta, I. Vayá, T. Gustavsson, A. B. Kotlyar, D. Zikich, P. Šket, J. Plavec, D. Markovitsi, *J. Phys. Chem., C* **116** (2012) 14682 (https://dx.doi.org/10.1021/jp303651e)
13. A. Banyasz, L. Martinez-Fernandez, C. Balty, M. Perron, T. Douki, R. Improta, D. Markovitsi, *J. Am. Chem. Soc.* **139** (2017) 10561 (https://dx.doi.org/10.1021/jacs.7b05931)
14. R. Improta, *Chem. Eur. J.* **20** (2014) 8106–8115 (https://dx.doi.org/10.1002/chem.201400065)
15. C. J. Lech, A. T. Phan, M.-E. Michel-Beyerle, A. A. Voityuk, *J. Phys. Chem., B* **119** (2015) 3697 (https://dx.doi.org/10.1021/jp512767j)
16. Y. Zhao, D. G. Truhlar, *Theor. Chem. Acc.* **120** (2008) 215 (https://dx.doi.org/10.1007/s00214-007-0401-8
17. T. Yanai, D. P. Tew, N. C. Handy, *Chem. Phys. Lett.* **393** (2004) 51 (https://dx.doi.org/10.1016/j.cplett.2004.06.011)
18. A. D. Becke, *J. Chem. Phys.* **98** (1993) 5648 (https://dx.doi.org/10.1063/1.464913)
19. D. Jacquemin, E. A. Perpete, I. Ciofini, C. Adamo, R. Valero, Y. Zhao, D. G. Truhlar, *J. Chem. Theory Comput.* **6** (2010) 2071 (https://dx.doi.org/10.1021/ct100119e)
20. G. A. Petersson, A. Bennett, T. G. Tensfeldt, M. A. Al-Laham, W. A. Shirley, J. Mantzaris, *J. Chem. Phys.* **89** (1988) 2193 (https://dx.doi.org/10.1063/1.455064)
21. A. D. McLean, G. S. Chandler, *J. Chem. Phys.* **72** (1980) 5639 (https://dx.doi.org/10.1063/1.438980)
22. G. A. Petersson, M. A. Al-Laham, *J. Chem. Phys.* **94** (1991) 6081 (https://dx.doi.org/10.1063/1.460447)
23. R. Krishnan, J. S. Binkley, R. Seeger, J. A. Pople, *J. Chem. Phys.* **72** (1980) 650 (https://dx.doi.org/10.1063/1.438955)
24. M. J. Frisch, J. A. Pople, J. S. Binkley, *J. Chem. Phys.* **80** (1984) 3265 (https://dx.doi.org/10.1063/1.447079)
25. T. H. Dunning Jr, *J. Chem. Phys.* **90** (1989) 1007 (https://dx.doi.org/10.1063/1.456153)
26. A. Schäfer, H. Horn, R. Ahlrichs, *J. Chem. Phys.* **97** (1992) 2571 (https://dx.doi.org/10.1063/1.463096)
27. *Gaussian 09, Revision A.02*, Gaussian, Inc., Wallingford, CT, 2016
28. T. Lu, F. Chen, *J. Comput. Chem.* **33** (2012) 580 (https://dx.doi.org/10.1002/jcc.22885)
29. T. Lu, F. Chen, *J. Mol. Graph. Model.* **38** (2012) 314 (https://dx.doi.org/10.1016/j.jmgm.2012.07.004).